Molecular Dynamics Study of the Transfer of Iodide across Two Liquid/Liquid Interfaces

Pedro Alexandrino Fernandes, M. Natália D. S. Cordeiro,* and José A. N. F. Gomes

CEQUP/Dept. Química, Faculdade de Ciências da Universidade do Porto, Rua do Campo Alegre 687, 4069-007 Porto, Portugal

Received: May 24, 1999; In Final Form: July 29, 1999

This work focuses on the study of the properties of two liquid/liquid interfaces, the H_2O/2-heptanone and the H_2O/iso-octane interfaces, and on the transfer of the iodide ion across them. A detailed study of the properties of the first interface was already reported *(J. Phys. Chem. B,* 1999, in press). The iso-octane liquid is a hydrophobic analog of the very hydrophilic 2-heptanone, and the properties of the H_2O/iso-octane interface are analyzed here and compared with the ones obtained for the H_2O/2-heptanone system. It is shown that the basic features characterizing the interface structure (such as the non-existence of a mixed solvent region or the broadening of the sharp interface by capillary waves) are almost unaffected by the change of the hydrophilic nature of the organic solvent. A new method is proposed to calculate more accurately properties which depend on the distance to the interface. In the case of density profiles, the application of this method reveals that both liquids are packed in layers against the interface. This structural pattern, not detectable using classical methods, allows us to understand the reason for the oscillations in the density profiles calculated perpendicularly to the interfacial plane, an unsolved problem for more than one decade. The free energy profiles for the transfer of iodide across the two interfaces are computed and compared. In both cases they show a monotonous decrease in the free energy as the ion moves from the organic solvent into water. The value obtained for the Gibbs free energy of transfer is in good agreement with the available experimental data. In addition, the mechanism of the ion transfer is investigated. The process of transfer from the water phase to the organic one and the reverse process involve, in both cases, the formation of a water cone that connects the hydration sphere of the ion to the water phase. This water cone is a chain of molecules that can be as long as 10 Å. After the disruption and retraction of the water cone, the ion in the organic solvent retains part of its first hydration shell. The mechanism of the transfer through both interfaces is, in qualitative terms, very similar, although the ion transfer free energies are very different, as expected considering the relative hydrophilicity of the present solvents.

I. Introduction

The transfer of ions across the interface between two immiscible liquids is an important chemical process, playing a major role in many chemical and biological phenomena. Phase transfer catalysis,[1] the kinetics of ion extraction,[2] or drug delivery in pharmacology[3] are some of the problems where the ion transfer process is a fundamental key step.

Despite the importance of this electrochemical process, our knowledge about the mechanism of the ion transfer is still very scarce. In fact, to clarify this kind of mechanism, a clear description of the properties of the liquid/liquid interface is needed. In the last few years, new experimental techniques have significantly contributed to our understanding of the microscopic properties of liquid interfaces.[4−8] At the same time, theoretical methods such as computer simulations have provided new useful insights about these systems.[9−15] However, a lot can still be done in the theoretical study of the ion transfer process. In this work we address not only the problem of the structural characterization of an interface but also the process of ion transfer by resorting to the molecular dynamics (MD) technique.

To begin with, some results of a MD simulation of the H_2O/iso-octane interface are presented. This system was chosen because iso-octane (ISOC) corresponds to the hydrophobic analog of 2-heptanone (HPT2), as the only difference between them is the replacement of the polar oxygen of the ketone by a methyl group. On the other hand, HPT2 is one of the most hydrophilic liquids immiscible with water that is commonly used in ion transfer processes. In fact, the solubility of water in HPT2 (8.3% (mol/mol)) is considerably high for such an immiscible liquid. Thus, direct comparison of the properties of both interfaces can shed some light into the influence of the hydrophobicity of the organic solvent on the structure of the interface. The study of the H_2O/iso-octane interface is also very important for the interpretation of the results obtained on the ion transfer simulations.

In Section II below, a brief description of the potentials as well as the methods used on the simulations is presented. Section III refers to the results of the study of the net H_2O/iso-octane interface. These results are analyzed and compared to the ones previously obtained for the H_2O/HPT2 interface.[14] A new method for the calculation of the density profile fluctuations perpendicular to the interface is outlined. This method enables us to understand the reason for the fluctuations in the density profiles, a problem that remained unsolved for more than one decade. Section IV describes the simulation of the iodide transfer across both interfaces. In that section, the free energy profile of the ion transfer and its mechanism are also discussed. In the last section, we summarize the conclusions achieved in this work

* Corresponding author.

10.1021/jp9916945 CCC: $18.00
Published on Web 10/04/1999

and analyze their implications to the current knowledge of the structure of liquid interfaces and ion transfer processes.

II. Computational Model

A. Molecular Models and Potentials. The water molecules were described through the well-known SPC model.[16] For the HPT2 and ISOC molecules, united atom models were employed in which the CH_n ($n = 1,2,3$) groups are replaced by one site centered on the C atom. Thus, both molecules are represented by an eight interaction site model.

All bond lengths were held fixed by applying the SHAKE algorithm.[17] This allows us to integrate the equations of motion with a time step of 2 fs, resulting in a better sampling of the configurational space. Preliminary checks confirmed that these bond constraints did not affect the properties studied here. All bond angles and dihedrals were considered flexible using the CHARMm intramolecular force field.[18]

The applied intermolecular potentials are pairwise additive potentials that include coulombic and Lennard-Jones (LJ) terms with parameters taken from the AMBER force field,[19] except in the cases referred below. In a previous work,[20] the accuracy of the CHARMm and AMBER force fields in the calculation of the density and heat of vaporization of pure HPT2 was compared. It was concluded that the AMBER intermolecular force field led to a slightly better agreement with experimental data. Concerning the intramolecular force field the bond and angle potentials of CHARMm and AMBER are basically equivalent, although the torsional potentials of CHARMm are somewhat more specific. This observation motivated us to choose the CHARMm intramolecular forcefield. For the HPT2 molecule, atomic charges were derived from quantum calculations, as previously reported.[20] The ISOC molecule is a saturated hydrocarbonide and, therefore, natural null charges were attributed to all its interaction sites. It should be also said that, for all interactions between different species, standard geometric combination rules were adopted to obtain the needed LJ parameters.

B. Method. The H_2O/HPT2 system as well as the H_2O/ISOC system were modeled initially by two rectangular boxes. In the case of the H_2O/HPT2 system, one of the boxes contained a mixture of 168 HPT2 molecules with 15 water molecules, and the other one contained 794 water molecules. In this way, the experimental concentration of water in saturated HPT2 was achieved. In the case of the H_2O/ISOC system, the first box had only 168 ISOC molecules, since the solubility of water in ISOC is too small to be considered, and the other box contained also 794 water molecules.

All these boxes had a cross section of 25 Å × 25 Å and a length that reproduces the density of the corresponding pure liquids (respectively, 0.997 g/cm^3 for water, 0.8124 g/cm^3 for HPT2, and 0.6980 g/cm^3 for ISOC).

To enable volume variations, all simulations were performed at 300 K and 1 bar in the NPT ensemble, using the Nosé−Hoover thermostat and barostat.[21,22] It should be noticed that, as the interface density is a priori unknown, if the box volumes were fixed this might induce serious restrictions in the formation of the interface.

A time of 300 ps was first used to equilibrate the two boxes containing the separate water and saturated HPT2 liquids. Then, the two boxes were brought together into one single box with the same cross section (from now on, the XY plane in our internal frame). In this process the volume was kept fixed and the equilibrium was reached by slowly turning on the interactions between the two liquids. An equilibration of 150 ps in the NPT ensemble was performed afterwards.

A similar procedure was applied to obtain the NPT-equilibrated H_2O/ISOC biphasic system. The last configuration of the NPT simulation was then used as the starting configuration for a new NPT simulation of 900 ps, from which the averaged properties of the H_2O/ISOC interface were taken.

To study the ion transfer process, the iodide ion was placed initially in the bulk water phase of the H_2O/HPT2 system, at 10 Å from the interface, and in the bulk ISOC phase 5 of the H_2O/ISOC system, at 25 Å from the interface. The ion interactions were smoothly increased from zero to their real values. NPT equilibration runs of 75 ps were found to be enough to equilibrate both interface systems. Notice that during those runs the ion was held fixed on its initial position while the rest of the system was free to move.

For the ion transfer process, a good approach to the reaction coordinate is the distance of the ion from the interface and, to calculate its free energy profile, the conventional constrained molecular dynamics method[23] was applied. The ion was kept fixed in its initial position during the first 2.5 ps and the forces acting on the ion were collected. Then, the ion was moved apart 0.05 Å along the reaction coordinate and a new sampling of 2.5 ps was carried out, collecting again the forces acting on the ion. This procedure was repeated until the ion reached the other bulk phase.

Similar procedures were successfully applied and proven to be very useful in the study of transfer processes of ions and neutral species across liquid/liquid interfaces.[24−26]

In the case of H_2O/HPT2 system, the ion transfer was performed in both directions, namely $H_2O \rightarrow$ HPT2 and HPT2 $\rightarrow H_2O$. In the case of the H_2O/ISOC system, only the spontaneous ISOC $\rightarrow H_2O$ process was simulated since it might seem somewhat unrealistic to transfer an ion from water to a saturated hydrocarbonide.

For the H_2O/HPT2 system, the free energy profile system was averaged over a 2 ns trajectory, and for the H_2O/ISOC system over a 1.75 ns trajectory. To allow for the relaxation of the solvent, after each ion displacement, a trajectory of 2.5 ps was carried out, but only the last 2 ps were used to produce the average forces. The 0.5 ps equilibration period was checked to be enough to equilibrate the solvent around the ion after such a small displacement.

Considering that the Z-axis of our internal frame is perpendicular to the interfacial plane, the free energy difference between a state where the ion is located at z_i and a reference state, z_{ref}, is obtained through[23,25,26]

$$\Delta G(z_i) = G(z_i) - G(z_{ref}) = -\int_{z_{ref}}^{z_i} \langle ||\vec{F}_z|| \rangle_{z'} \, dz' \qquad (1)$$

where $||\vec{F}_z||$ corresponds to the z component of the force acting on the ion, and $\langle ... \rangle_{z'}$ represent NPT averages with the ion fixed in the z' position. In this work, z_{ref} was considered to be the position of the ion in the bulk water phase.

All simulations were carried out using the DL_POLY MD package.[27]

The integration of the equations of motion was done using the Verlet leapfrog algorithm with a timestep of 2 fs. Periodic boundary conditions were set in all three directions, thus creating two liquid/liquid interfaces in the box. In these cases, the simulation box must be long enough to avoid interactions between the two interfaces and any perturbation of the bulk liquids. In our system, the initial separation of the interfaces was 38 Å along the water phase and 61.68 Å along the HPT2

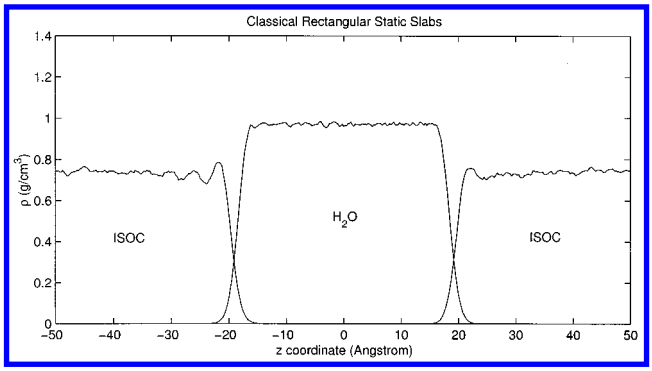

Figure 1. Density profile of the H_2O/ISOC system calculated using the classic rectangular static slabs method.

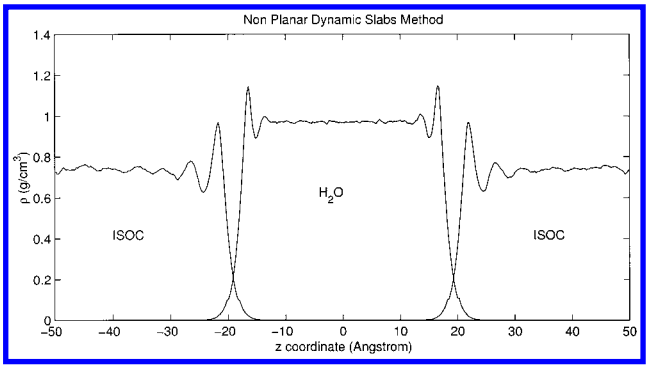

Figure 2. Density profile of the H_2O/ISOC system calculated using the non planar dynamic slabs method.

phase (and longer in the case of ISOC, due to the more reduced density), i.e., 3.1 and 5.0 times greater than the long-range cutoffs used, what seems quite enough to prevent interfacial correlations.

Long-range forces were taken into account following an Ewald scheme with tinfoil boundary conditions. A molecular spherical cutoff of 12.25 Å for the real part of the Ewald energy was applied. For the short-range interactions a cutoff of 10 Å was used.

The use of the Ewald method in the simulations of an electrically charged system normally raises the question of whether the electroneutrality of the system is preserved or not. However, the method includes a term corresponding to a background with a charge opposite in sign to the system's charge, which makes the overall system neutral.[28,29] Therefore, the Ewald method is suitable even to handle the long-range forces of electrically charged systems.

To increase the speed of the MD simulations, the forces between pairs at distances larger than 10 Å were evaluated by a multiple timestep algorithm[30] with a frequency of actualization of 10 fs. Previous tests have shown that this algorithm leads to a good energy conservation without the thermostat apart from not affecting the properties of the system.

III. Results

A. Density Profiles. *1. The Non Planar Dynamics Slabs Method.* The density profile along an axis normal to the interfacial plane provides useful information about the average extension of the interfacial zone. The method commonly employed to determine it divides the simulation box in rectangular slabs parallel to the interfacial plane, with a thickness of about 1 Å. From now on in this paper this method will be referred as the classic static rectangular slabs (CSRS) method.

The density profile of the H_2O/ISOC system computed by the CSRS method is shown in Figure 1. Notice that the coordinates of all molecules in the Z-axis were corrected at each integration step according to the fluctuations of the center of mass of the system (the origin of the Z-axis was located at the *z* coordinate of the system's center of mass).

Since the pioneering work of Linse[9] that somewhat regular oscillations have been observed on the density profiles, although their origin remained unclear until now. The smoothing of the oscillations with increasing sampling seemed to indicate that they result from the statistical uncertainty of the simulations, although the idea of the existence of a layering effect near the interface was never excluded.[9,11−13,31−34] In this work, we propose a new method to compute density profiles that will elucidate the nature of these density oscillations.

The liquid/liquid interfaces are neither static nor planar, but very corrugated and broadened by capillary waves. The molecules inside a given slab will have fixed distances in relation to the average interface position (excluding displacements inside the slab). However, their distances to the instantaneous position of the interface will vary according to the fluctuations of the interface position. Averaging some property of the molecules inside a given slab will result in an accumulation of values which, indeed, does not correspond to the exact values that should be attained at the same distance from the interface. Therefore, if the property being averaged strongly depends upon the interface location, the use of static rectangular slabs should be avoided. This problem can become quite dramatic for oscillatory properties with a wavelength of the same order of magnitude of the interface position fluctuations. In fact, the anomalous accumulation of values coming from oscillations in opposite phases may cancel the real oscillations of the property being analyzed. As it will be seen below, this is indeed the case for the structural oscillations appearing in the density profiles.

To overcome the problem referred to above, the XY plane was divided into 4×4 equal square areas with a side of about 6.25 Å and, in each square area, the location of the molecules with the largest value of *z* (largest protrusion from their phase into the other phase) was calculated. This allows us to define local interface positions.

For the H_2O/ISOC system two interfacial surfaces were defined in this way, one corresponding to the surface defined by the position of the water local interfaces and the other one defined by the positions of the ISOC local interfaces. This procedure was repeated at each time step since the interface constantly changes its location and shape. The properties of water that depend on the distance to the interface are then separately computed in slabs parallel to the ISOC interface (the hydrophobic wall that the water phase feels). In the same way, the ISOC properties are also separately computed in slabs parallel to the water interface (the organophobic wall that the ISOC phase feels).

The present method seems to be appropriate to obtain average properties that depend on the distance from the interface and avoids the accumulation of values in a non-phased manner. This new method will be referred from now on as the non planar dynamics slabs (NPDS) method.

The density profile of the H_2O/ISOC system calculated by the NPDS method is shown in Figure 2. It is clear from this picture that a first water layer is packed against the ISOC phase. A second water layer is still visible, due to the packing of water against the first layer. Similarly, the ISOC phase presents a pronounced first peak corresponding to a first ISOC layer that is packed against the water phase. This packing effect propagates

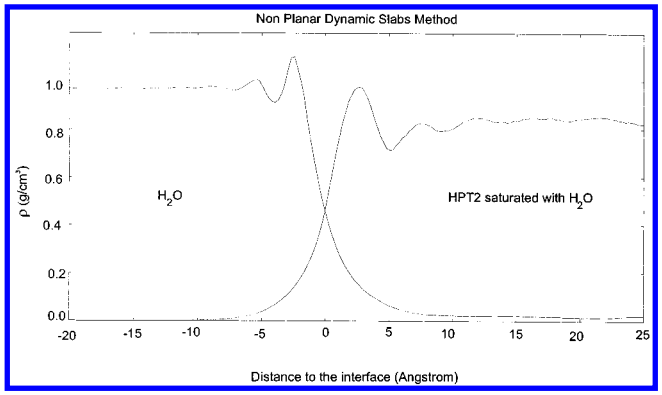

Figure 3. Density profile of the H_2O/HPT2 system calculated using the non planar dynamic slabs method. The right side of the density profile was accumulated into the left side to improve the statistics. Note that the peaks remain well defined, although the fluctuations associated to the uncertainty of the calculation almost disappear.

more strongly into the bulk ISOC phase than into the water phase, what might be explained by the different shape of the molecules. By increasing the sampling the amplitude of those structural peaks does not decrease, but the shorter wavelength oscillations become smoother. Thus the latter oscillations may undoubtedly be associated to the uncertainty of the simulation and the former ones to the packing of the liquids against the interface. Here, it should be emphasized that a similar behavior was obtained for the H_2O/HPT2 density profile using the NPDS method. Indeed, a very long simulation of the H_2O/HPT2 system was performed (2.25 ns) and the obtained density profile is depicted in Figure 3. The symmetry of the system was used to improve the statistics. This density profile can be compared with the one obtained in a previous work[14] where the old CRSM was used (i.e., a density profile analogous to the one presented in Figure 1). So, this behavior holds on, independently of the hydrophobic nature of the organic solvent. We now believe that the oscillations usually observed in the density profiles are finally understood.

At this point, it is interesting to compare the above results with the results of the simulations of solid/liquid interfaces. The density profiles obtained for water in contact with a solid planar interface are very similar to the ones achieved here with the NPDS method. Both exhibit at least two distinguishable water layers, followed by oscillations of shorter wavelength due to the noise of the calculations.[35−39] As the solid/liquid interfaces are static and planar, the artifacts caused by the CSRS method are not seen as they are on liquid/liquid interfacial systems. A recent simulation of the H_2O/Hg interface[40] also revealed an oscillatory density profile, with three distinct water layers and an oscillatory structure for Hg throughout the Hg phase. The high surface tension of the H_2O/Hg interface (375 dyn/cm[41]) makes this interface much more static and planar than any other liquid/liquid interface, and the CSRS method is thus capable of detecting the layering structure of both liquids.

In the future, the fast-increasing computational resources and new advances in the field of numerical simulations, will allow much larger simulated systems. However, using much larger interfacial areas will predictably produce larger amplitudes in the positional oscillations of the local interfaces, and will enhance the artifacts coming from the use of the CSRS method. Notice that, according to the capillary wave formalism, the mean square fluctuations in the interface position are proportional to the logarithm of the interfacial area (see eq 6 below). Early works have shown that the increase of the interfacial area makes the density oscillations smoother or even unnoticeable when computed by the old CSRS method.[42] Although more computationally demanding, the use of the NPDS method will therefore become an indispensable tool for averaging properties that depend on the distance to the interface.

2. The H_2O/ISOC Interface. As can be seen in Figure 2, the H_2O/ISOC average density profile shows two stable interfaces, indicating that the potential models successfully describe the formation of the interfaces. The average bulk liquid densities are in good agreement with the experimental data. The average water density in a central slab corresponding to $-12 \le z \le 12$ is 0.970 g cm^{-3} (which corresponds to the density of the SPC water model[43]) and, on the other hand, the average ISOC density in slabs corresponding to $-49 \le z \le -25$ and $25 \le z \le 49$ is 0.74 g cm^{-3} (the experimental value is 0.70 g cm^{-3} [41]). The Gibbs dividing surface can be located at the middle point where the density of both liquids falls to one half of their bulk values. With this criteria the interfaces are located at $z = -19.0$ Å and $z = +19.1$ Å.

The average density profile does not allow us to distinguish a thick interface (i.e., an interface with a gradual change in composition from one bulk liquid to the other) from a sharp interface (i.e., an interface without a mixing zone but with a position that fluctuates in time). More detailed information about the interface structure can be obtained by computing the positions and widths of the interface as a function of the interfacial area. These may vary between the whole box cross section to a smaller meaningful square area with a side corresponding to the ISOC molecular length (about 6.5 Å). A clear explanation of the method used on those calculations may be found elsewhere.[9,11,14]

The interface position and width may be defined as follows:

$$W_{ij}^{\text{left}} = \max(z_{ij})(\text{ISOC}) - \min(z_{ij})(\text{H}_2\text{O}) \qquad (2)$$

$$H_{ij}^{\text{left}} = \frac{1}{2}\left(\min(z_{ij})(\text{H}_2\text{O}) + \max(z_{ij})(\text{ISOC})\right) \qquad (3)$$

for molecules on the left side of the simulation box, and

$$W_{ij}^{\text{right}} = \max(z_{ij})(\text{H}_2\text{O}) - \min(z_{ij})(\text{ISOC}) \qquad (4)$$

$$H_{ij}^{\text{right}} = \frac{1}{2}\left(\max(z_{ij})(\text{H}_2\text{O}) + \min(z_{ij})(\text{ISOC})\right) \qquad (5)$$

for molecules in the right side of the simulation box.

In these equations, z_{ij} corresponds to the z coordinate of the molecular sites that belong to the ij fractional area of the XY plane and H_{ij}, W_{ij} are, respectively, the position and the width of the ij fractional interface.

The XY plane was divided into 1, 4, 9, and 16 equal fractional areas and the interfacial positions and widths were independently calculated within them. The results obtained are plotted in Figure 4.

Equations 2 and 4 show us that a positive width corresponds to an interpenetration of the molecules of one liquid into the other, and a negative width corresponds to an effective separation of both phases. From the inspection of Figure 4, it is clear that as the surface area decreases the average width of the interface becomes negative, indicating that the two phases do not mix. The behavior of the interface width distribution is consistent with a sharp interface, without mixing at a molecular level (width < 0 for small surfaces) but very corrugated, what can be inferred from the fact that its width becomes positive for the largest surface areas. This gives us a picture of an interface where relatively large amounts of each phase protrude

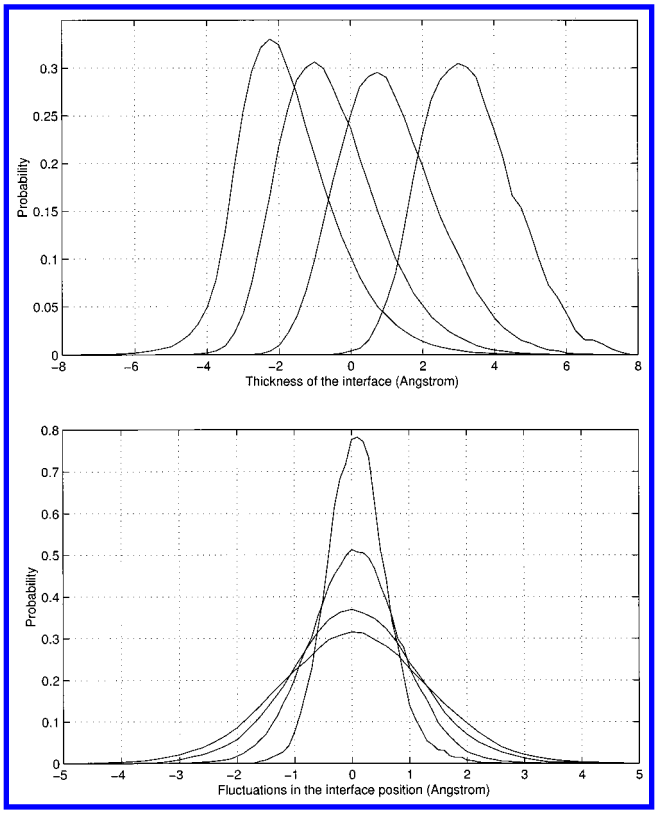

Figure 4. Top: Probability distribution of the width of the H_2O/ISOC interface, calculated using different surface areas. The lines correspond, from right to left, to $N = 1$, 2, 3, and 4, respectively. Bottom: Probability distributions for the fluctuations of the position of the H_2O/ISOC interface, calculated using different surface areas. The four lines correspond, from the sharpest to the broadest, to $N = 1$, 2, 3, and 4, respectively.

into the other, but without solvation of isolated molecules of one phase by the other. The interfacial corrugation can be also detected from the distributions of the position of the fractional interfaces (Figure 4, bottom), as these become broader with the decrease of the fractional interfacial areas.

At this point, it is important to compare the above results with the ones obtained for the H_2O/HPT2 system.[14] The average width of the H_2O/HPT2 interface was determined to be +1.0 Å for the smallest surface areas considered. In that system, water and HPT2 interpenetrates up to 1.0 Å in average, i.e., less than one water molecular diameter. In the H_2O/ISOC system the average width of the interface calculated for the smaller surface areas is −1.0 Å, corresponding to an effective separation of both phases by a gap of 1.0 Å. Changing the nature of the organic solvent (from the very hydrophobic ISOC to the very hydrophilic HPT2) only slightly modifies the average interpenetration of the phases (from −1.0 to +1.0 Å). This means that the extension of the mixed region (which is, at best, almost nonexistent) is practically not affected by the hydrophilic nature of the organic solvent. Thus it seems that the thickness of most water/organic liquid interfaces should be, in general, analogous to the ones obtained here. Of course, one might question the validity of this statement as it is based on the results of only two particular interfaces. Notice, on the other hand, that to get a more visible enlargement of the mixed region, HPT2 should be replaced by a much more hydrophilic solvent and this will result in a mixing of the two phases.

Another interesting aspect is the description of the fluctuations of the interface position in terms of capillary waves. From the capillary wave theory, the surface tension of the interface (γ_c)

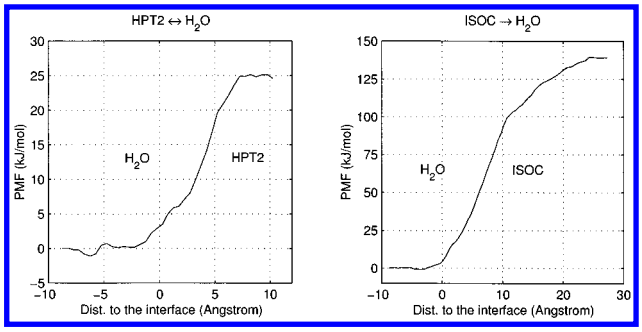

Figure 5. Potential of mean force for the iodide transfer across the H_2O/HPT2 (left) and the H_2O/ISOC (right) interfaces.

may be related with the interface width arising from the thermal fluctuations superimposed under an infinitely sharp surface.[44] Neglecting gravitational effects, this relation is given by

$$\langle \zeta^2 \rangle = \frac{k_B T}{2\pi\gamma_c} \ln\left[\frac{L}{l}\right] \qquad (6)$$

In this equation, L and l are the upper and lower cutoffs of the capillary wave spectrum, respectively, and $\langle \zeta^2 \rangle$ is the mean square fluctuation of the surface location away from its equilibrium position. The lower cutoff is usually chosen to be the diameter of the organic molecules, and the upper cutoff, L, is determined by the system size.

Using the mean square deviation of the surface position distributions obtained with the smaller surface areas and $l =$ 6.5 Å, a value of 54.4 ± 0.1 dyn/cm is obtained for γ_c. l was chosen to be the average length of the ISOC molecule, although γ_c is not very sensitive to it.

The experimental surface tension for water against the linear *n*-octane is 50.8 dyn/cm.[41] Considering the physical and chemical similarity between the two isomers, i.e., iso-octane and *n*-octane, it is reasonable to believe that the surface tension of both against water should be very similar. One should remember that the surface tension on those systems is more influenced by the nature of their molecules than by the small differences on their shape or size. For instance, the surface tension of the H_2O/hexane interface is 51.1 dyn/cm,[41] a value pretty close to the one obtained in the case of the H_2O/*n*-octane interface. Thus, it might be expected that the γ_c of the H_2O/iso-octane system should be very similar to the H_2O/*n*-octane γ_c, meaning that our results are very realistic. One can then conclude that, at least for the systems considered here, the capillary wave theory gives a reasonable quantitative description of the fluctuations in the position of the interface.

B. The Iodide Transfer. In this section, the potential of mean force (PMF) for the transfer of an iodide ion through the H_2O/HPT2 or the H_2O/ISOC interfaces and the mechanism of this transfer are analyzed.

1. The Potential of Mean Force. Figure 5 shows the results of the PMF calculations carried out for the ion transfer across both interfaces. As can be seen, the free energy shows no drift at the beginning (in bulk water) and at the end of the ion transfer (in bulk HPT2 or ISOC), confirming that the reaction coordinate is fully investigated.

The PMFs in Figure 5 have a very similar profile. They show a monotonous increase in the Gibbs free energy as the ion leaves the water liquid and enters the organic liquid. This simply reflects the greater stability of the ion in water, and clearly resembles the pioneering PMF obtained by Benjamin for an ion transfer across an interface between two Lennard-Jones model liquids.[45]

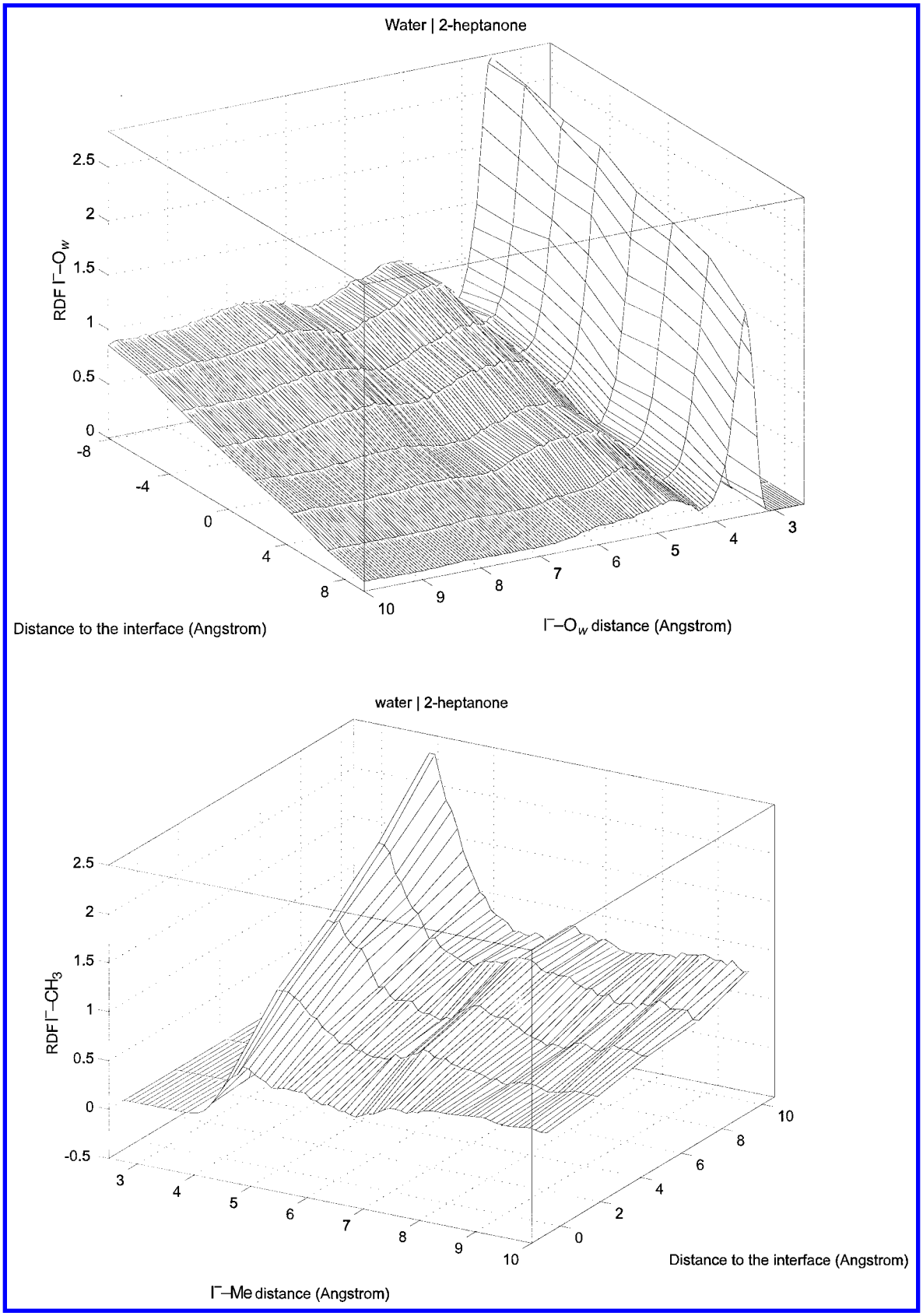

Figure 6. I^-—O_w (top) and I^-—Me (bottom) radial distribution functions for the water/HPT2 system. Both functions are normalized by the correspondent bulk solvent densities.

When the ion is still in the water phase the change in free energy is quite small and it increases significantly only after the ion reaches the organic phase.

The Gibbs free energy for the transfer of I^- through the HPT2/H_2O interface is -24.7 ± 3.4 kJ/mol (average value for the transfer in both directions, hysteresis = 5.8 kJ/mol), a result in fair agreement with the one (−21.9 kJ/mol) recently obtained experimentally.[46] As far as we know, there are no experimental results for the free energy of the I^- transfer across the H_2O/ISOC interface. However, the value obtained here for that

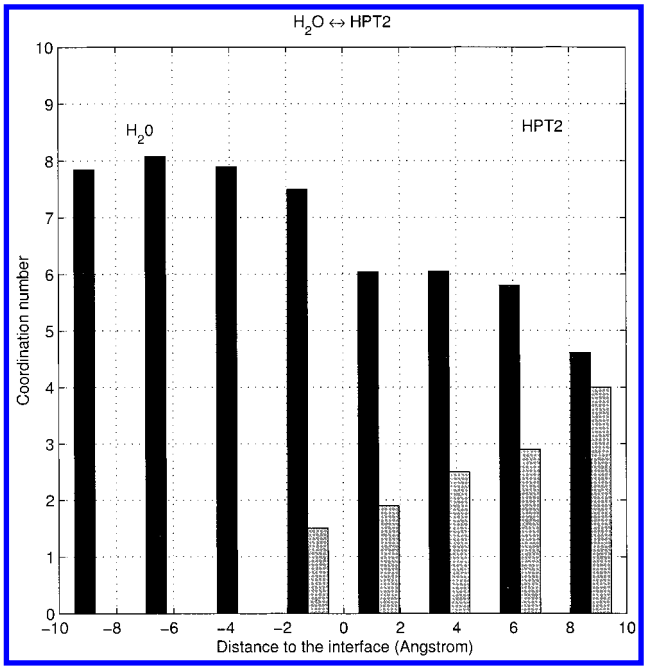

Figure 7. Coordination numbers for the first hydration shell of I^- in the water/HTP2 system. Black bars correspond to the number of coordinated water molecules and gray bars correspond to the number of HPT2 coordinated molecules.

transfer (-139.0 ± 6.3 kJ/mol) seems very reasonable, as it should be much more difficult to transfer an ion from water to ISOC than to HPT2, due to the much smaller polarity of ISOC. The statistical errors associated to the transfer free energies were calculated through a block means analysis.

2. The Mechanism of the Ion Transfer. More insight into the exchange of the ion's solvation shell during the transfer process can be obtained by examining the I^- associations in the two systems studied. Thus, radial distribution functions (RDFs) for the $I^-{-}O_w$ pair were computed for both interfaces (O_w denotes to the H_2O oxygen). In the case of the H_2O/HPT2 system the $I^-{-}$Me RDF was also calculated (Me being the terminal methyl group adjacent to the ketone oxygen), as I^- is mostly solvated by HPT2 through this positively charged methyl group. In fact, the carbonyl carbon of HPT2, although having a higher positive charge, is too hidden by the methyl groups of HPT2 to solvate the ion. In addition, RDFs for the $I^-{-}$Me′ pairs, where Me′ represents any of the ISOC sites, were computed for the H_2O/ISOC system. This choice was motivated by the fact that the RDFs for I^- obtained with any of the ISOC sites were all very similar. However, the RDF for the association of I^- with the linear extremity of ISOC was somewhat more demarked than the others. The RDF for I^- and the branched tail of ISOC did not reveal a significantly more pronounced first peak than with the other methyl groups since the interaction with such a large branched tail precludes other interactions.

All RDFs were obtained by applying our new NPDS method. The simulation cell was divided into slabs of 2.5 Å thickness and, then, separate RDFs are computed with the I^- ion inside each slab. By resorting to a triangle-based linear interpolation of the data points in each slab, three-dimensional RDFs are defined which are functions of both the pair distance and the interface distance. Each RDF has been normalized by the respective bulk density and integrated to estimate the number of neighbors inside the ion's first coordination shell. The RDFs and coordination numbers are plotted in Figures 6, 7 and 8, 9, respectively, for the H_2O/HPT2 system and for the H_2O/ISOC system.

One should note that, as the ion goes from water to HPT2, its second solvation shell almost disappears but its first shell is partially retained, even in bulk HPT2. It is also important to note that, when the ion moves from HPT2 to water, its first solvation shell only becomes complete after the ion crosses the interface. From the results reported in Figure 7, it can be seen that the I^- ion retains an average of 4.6 water molecules in the organic phase in a mixed solvation shell which also contains an average of 4.0 methyl groups. In previous simulations of I^- in saturated HPT2 (a system of 232 HPT2 molecules plus 21 water molecules and one I^-), the formation of a mixed solvation sphere of 3.2 water molecules plus 5.1 HPT2 molecules was observed. This means that the transferred ion drags some water into the organic phase, a phenomenon well documented theoretically and experimentally.[47,48]

The second peak in the $I^-{-}O_w$ RDF almost vanishes in bulk HPT2, meaning that the ion is surrounded by a single hydration shell. Experimentally, it is well known that the water content of the organic phase increases with the ion transfer process. Accurate numbers of coextracted water molecules from water to nitrobenzene by alkaline and alkaline-earth cations have been experimentally measured.[49−53] Water coextraction was also detected with other organic solvents, such as 4-methyl-2-pentanone, chloroform, or nitrobenzene−benzene mixtures.[54−57] Thus, the water dragging effect noticed in the present simulations seems to be in agreement with the experimental findings.

The $I^-{-}$Me RDF shows a first peak (see lower part of Figure 6) that augments as the ion moves into the HPT2 phase, i.e., the ion's first hydration shell is partially replaced by HPT2 molecules. The solvation of I^- by HPT2 begins at the interfacial zone and grows until a maximum of 4.0 neighbors when the ion reaches the bulk organic phase (vide Figure 7).

The solubility of water in ISOC is very small and, thus, the I^- ion is unhydrated in ISOC. From the $I^-{-}O_w$ RDF of the H_2O/ISOC system (Figure 8) it can be seen that the ion is not hydrated until it gets to a distance of about 10 Å from the interface. Afterwards, water molecules begin to form a hydration shell which is only complete when the ion reaches bulk water. The number of coordinated water molecules grows from 3.6 at the beginning of the formation of the ion's hydration shell to about 8 in bulk water (see Figure 9). The results presented in the next section will allow for a more clear interpretation of the formation of this hydration shell in bulk ISOC.

The $I^-{-}$Me′ RDF shows a ISOC coordination shell containing about 7 ISOC molecules that remains stable until the water molecules match the ion. Then, the first peak of this RDF monotonously decreases as the ion progresses towards the water phase. The replacement of all ISOC molecules by water molecules occurs only when the ion reaches the water phase. The exchange of the ion's solvation shell is clearly seen in Figure 9.

C. Formation of a Water Cone. By analyzing the animated trajectories of the simulations, it can be observed that when the ion crosses the interface and is moving towards bulk HPT2 it remains connected to the water phase through a water chain, until it reaches a distance from the interface of about 9 Å. Then the water chain disrupts and retracts, leaving, however, some water molecules in the organic phase hydrating the ion. The fraction of hydrogen-bonded water molecules in the water cone is clearly superior to the bulk average.

To study the degree of hydrogen bonding in the water cone the following criteria were used: a water molecule belongs to the coordination shell of another water molecule if their O−O distance is no greater than the first minimum of the O−O RDF

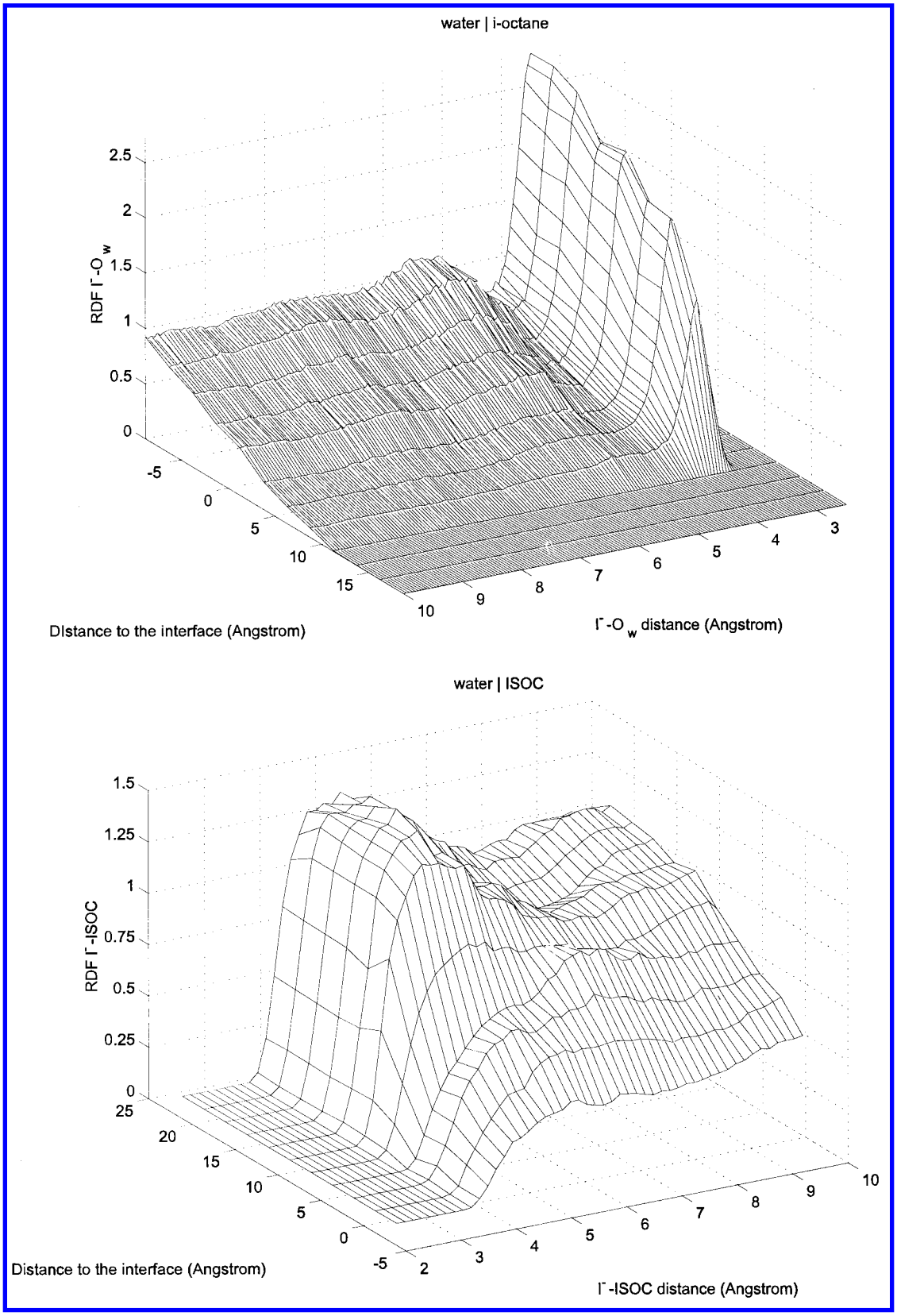

Figure 8. I^--O_w (top) and I^-−Me′ (bottom) radial distribution functions for the water/ISOC system. Both functions are normalized by the correspondent bulk solvent densities.

(3.5 Å). Furthermore, two water molecules establish a hydrogen bond if any H−O distance between them is no greater than the first minimum of the H−O RDF (2.4 Å). It was then calculated the fraction of water molecules inside the coordination shell of a given water molecule, which are hydrogen bonded to it, as a function of the distance to the interface. The results obtained for both systems studied here are depicted in Figure 10.

From Figure 10 it is clear that the degree of water hydrogen bonding is larger in the water cone than in bulk water. As the water molecules protrude into the organic liquid only the more

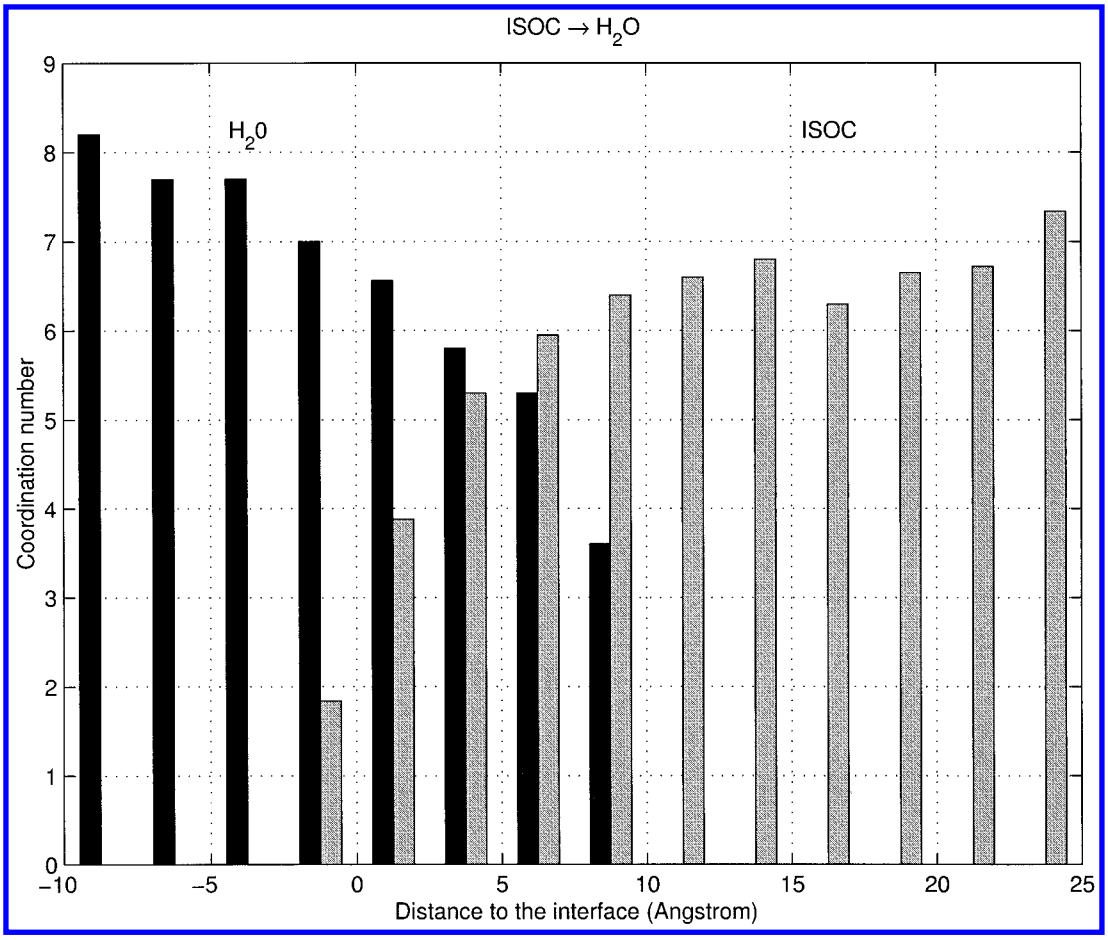

Figure 9. Coordination numbers for the first hydration shell of I^- in the water/ISOC system. Black bars correspond to the number of coordinated water molecules, and gray bars correspond to the number of ISOC coordinated molecules.

tightly bonded ones (i.e., the ones that are hydrogen bonded) may remain together in the organic phase. The same phenomenon, but to a lesser extent, is observed for the unperturbed second liquid/liquid interfaces (located at $z = -19.0$ Å in the H_2O/ISOC system and at $z = -19.4$ Å in the H_2O/HPT2 system).

The formation of this type of water cone was also observed in two other simulations of the ion transfer process through liquid/liquid interfaces, although in both cases the simulations could not be extended long enough in order to see the disruption and retraction of the water cone.[24,58]

For the reverse transfer processes, i.e., the ion starting from the bulk of the organic phase, the same phenomenon was observed. As the ion approaches the water phase, at a distance of about 9−10 Å a water capillary wave that gets close to the ion is attracted by it. Then the wave protrudes more deeply into the organic phase to match the ion, starts to hydrate it and the exchange of the ion's solvation shell begins. This explains the sudden formation of the ion's hydration shell in ISOC as it approaches the water phase at a distance of 10 Å (see Figure 8).

The formation of the water cone has some energetic cost since its water molecules establish a much smaller number of interactions with other water molecules than in the bulk or even in the interfacial region. In macroscopic terms, one can say that some work must be done to increase the interfacial area. This energetic cost is compensated by the strong iodide−water interactions *if* the ion is close enough to the water phase. In a series of test simulations, the ion was kept fixed at distances of 12.5 to 18 Å from the interface and, even after 350 ps, the capillary waves did not protrude into the organic phase to solvate the ion. Finally it should be stressed that, on the transfer of the I^- ion into the water phase, the amplitude of the water cone is very similar to the amplitude of the water cone on the reverse transfer process, before its disruption.

IV. Conclusions

In this work, the H_2O/ISOC interface was studied and compared to the H_2O/HPT2 interface. The results show that the exchange of the hydrophilic nature of the organic solvent only slightly affects the basic properties of the interface, like the inexistence of a mixed region or the broadening of the interface by capillary waves. From the comparison of our results with other studies of liquid/liquid interfaces[9−14,31−33] it can be said that the basic properties of the interfaces are all very similar and do not seem to depend very markedly either on the nature of the organic solvent or on the intermolecular potentials and the simulation methods employed. This fact gives more reliability to the studies of the liquid/liquid interfaces by computer simulations.

A new method was proposed to calculate, in a more correct and refined way, average properties that depend on the distance to the interface. The application of this new method to density profiles revealed the layering of the solvents against the interface and allowed us to understand the nature of the fluctuations in the density profiles, a subject of discussion for more than a decade.

The transfer processes of an iodide ion across the H_2O/ISOC and the H_2O/HPT2 interfaces was investigated. Potentials of

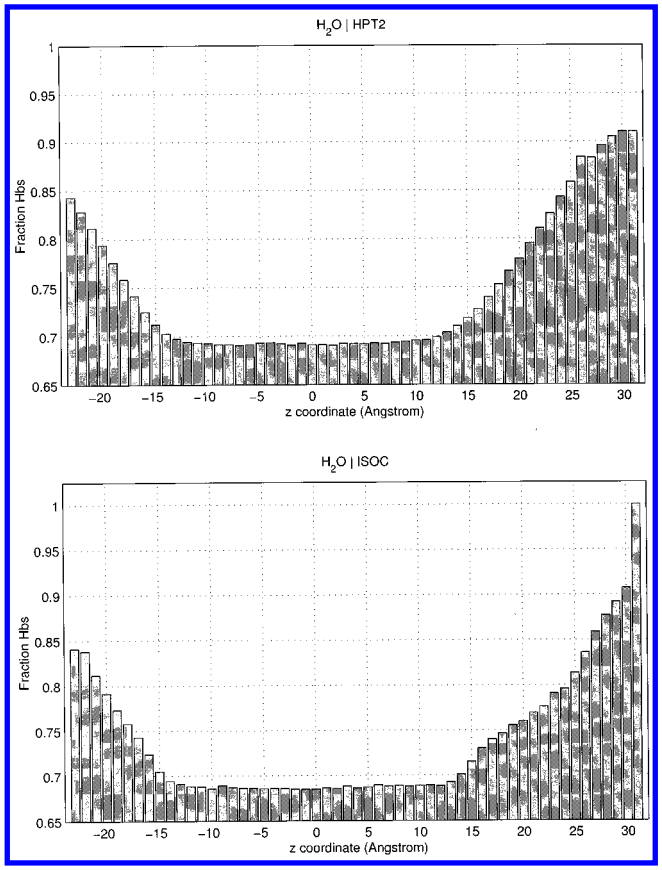

Figure 10. Fraction of water molecules inside a given water solvation shell that are coordinated via hydrogen bonds. Notice that the second liquid/liquid interfaces are located at $z = -19.4$ Å (top) and $z = -19.0$ Å (bottom).

mean force for the transfer processes were calculated and the estimated Gibbs free energies are in good agreement with the available experimental data. The profiles of the potentials of mean force are very similar for both transfers. They simply show a monotonous decrease of the free energy as the ion moves from the organic phase into the water phase, i.e., a barrier-free process. Of course, the free energy for the ion transfer from water to HPT2 is much smaller than the one from water to ISOC, a fact clearly explained by the relative polarity of the organic solvents. Both forward and reverse transfer processes involve the formation of a water cone that drags the ion from the organic solvent into the water phase. The coextraction of water molecules was also observed. After the transfer, the ion in the bulk organic phase still retains its partial hydration shell.

Acknowledgment. Financial support from Fundação para a Ciencia e a Tecnologia (Lisbon) through PRAXIS/PCEX/QUI/61/96 is acknowledged. P.A.F. thanks the Programa Praxis XXI for a doctoral scholarship (BD/9175/96). Helpful discussions with Prof. António F. Silva and Mr. Alfredo J. P. Carvalho of this department are gratefully acknowledged.

References and Notes

(1) Cunnane, V. J.; Schiffrin, D. J.; Beltran, C.; Geblewicz, G.; Solomon, T. *J. Electroanal. Chem.* **1988**, *247*, 203.
(2) Koryta, J.; Skalicky, M. *J. Electroanal. Chem.* **1987**, *229*, 265.
(3) Arai, K.; Ohsawa, M.; Kusu, F.; Takamura, K. *Bioelectrochem. Bioenerg.* **1993**, *31*, 65.
(4) Higgins, D. A.; Corn, R. M. *J. Phys. Chem.* **1993**, *97*, 489.
(5) Grubb, S. C.; Kim, M. W.; Rasing, T.; Shen, Y. R. *Langmuir* **1988**, *4*, 452.
(6) Conboy, J. C.; Daschbach, J. L.; Richmond, G. L. *J. Phys. Chem.* **1994**, *98*, 9688.
(7) Du, Q.; Superfine, R.; Freysz, E.; Shen, Y. R. *Phys. Rev. Lett.* **1993**, *70*, 2313.
(8) Eisenthal, K. B. *Annu. Rev. Phys. Chem.* **1992**, *43*, 627.
(9) Lynse, P. *J. Chem. Phys.* **1987**, *86*, 4177.
(10) Gao, J.; Jorgensen, W. *J. Phys. Chem.* **1988**, *92*, 5813.
(11) Benjamin, I. *J. Chem. Phys.* **1992**, *97*, 1432.
(12) Michael, D.; Benjamin, I. *J. Phys. Chem.* **1995**, *99*, 1530.
(13) Chang, T.; Dang, L. X. *J. Chem. Phys.* **1996**, *104*, 6772.
(14) Fernandes, P. A.; Cordeiro, M. N. D. S.; Gomes, J. A. N. F. *J. Phys. Chem. B* **1999**, *103*, 6290.
(15) *Molecular Dynamics: From Classical to Quantum Methods*; Balbuena, P. B., Seminario, J. M., Eds.; Elsevier: The Netherlands, 1999.
(16) Berendsen, H. J. C.; Postma, J. P. M.; van Gunsteren, W. F.; Hermans, J. In *Intermolecular Forces*; Pullman, B., Ed.; Reidel: Dordrecht, 1981; p 331.
(17) Ryckaert, J.; Ciccotti, G.; Berendsen, H. *J. Comput. Phys.* **1977**, *23*, 327.
(18) Brooks, B. B.; Bruccolery, R. E.; Olafson, B. D.; States, D. J.; Swaminathan, S.; Karplus, M. J. *J. Comput. Chem.* **1983**, *4*, 187.
(19) Pearlman, D. A.; Case, D. A.; Cadwell, J. C.; Seibel, G. L.; Sing, U. C.; Weiner, P.; Kollman, P. A. *AMBER4*; University of California: San Francisco, 1991.
(20) Fernandes, P. A.; Cordeiro, M. N. D. S.; Gomes, J. A. N. F. *J. Phys. Chem. B* **1999**, *103*, 1176.
(21) Hoover, W. G. *Phys. Rev.* **1985**, *A31*, 1695.
(22) Melchionna, S.; Ciccotti, G.; Holian, B. L. *Mol. Phys.* **1993**, *78*, 533.
(23) Paci, E.; Ciccotti, G.; Ferrario, M.; Kapral, R. *Chem. Phys. Lett.* **1991**, *176*, 581.
(24) Lauterbach, M.; Engler, E.; Muzet, N.; Troxler, L.; Wipff, G. *J. Phys. Chem. B* **1998**, *102*, 245.
(25) Chang, T.; Dang, L. X. *J. Chem. Phys.* **1998**, *108*, 2.
(26) Meyer, M.; Hayoun, M.; Turq, P. *J. Phys. Chem.* **1994**, *98*, 6626.
(27) Forrester, T. W.; Smith, W. *DLPOLY (2.1 version)*; CCLRC: Daresbury Laboratory, 1995.
(28) Figueirido, F.; Buono, G. S. D.; Levy, R. *M. J. Chem. Phys.* **1995**, *103*, 6133.
(29) Roberts, J. E.; Schnitker, J. *J. Chem. Phys.* **1994**, *101*, 5024.
(30) Forrester, T. W.; Smith, W. *Mol. Simul.* **1994**, *13*, 195.
(31) Pohorille, A.; Wilson, M. *J. Mol. Struct. (THEOCHEM)* **1993**, *284*, 271.
(32) Benjamin, I. *Chem. Rev.* **1996**, *96*, 1449.
(33) Michael, D.; Benjamin, I. *J. Electroanal. Chem.* **1998**, *450*, 335.
(34) Mitrinovic, D.; Zhang, Z.; Williams, S.; Huang, Z.; Shlossman, M. *J. Phys. Chem. B* **1999**, *103*, 1779.
(35) Lee, C. Y.; McCammon, J. A.; Rossky, P. *J. Phys. Chem.* **1984**, *80*, 4448.
(36) Spohr, E.; Heizinger, K. *Electrochim. Acta* **1988**, *33*, 1211.
(37) Heizinger, K. *Pure Appl. Chem.* **1991**, *63*, 1733.
(38) Raghavan, K.; Foster, K.; Mottakabir, K.; Berkowitz, M. *J. Chem. Phys.* **1991**, *94*, 2110.
(39) Schweighofer, K.; Xia, X.; Berkowitz, M. *Langmuir* **1996**, *12*, 3747.
(40) Bocker, J.; Gurskii, Z.; Heizinger, K. *J. Phys. Chem.* **1996**, *100*, 14969.
(41) *Handbook of Chemistry and Physics;* Weast, R. C., Ed.; CRC Press: Boca Raton, FL, 1989.
(42) Toxvaerd, S.; Stecki, J. *J. Chem. Phys.* **1995**, *102*, 7163.
(43) Berendsen, H. J. C.; Grigera, J. R.; Straatsma, T. P. *J. Phys. Chem.* **1987**, *91*, 6269.
(44) Weeks, J. D. *J. Chem. Phys.* **1977**, *67*, 3106.
(45) Benjamin, I. *J. Chem. Phys.* **1992**, *96*, 577.
(46) Cheng, Y.; Schiffrin, D. *J. Electroanal. Chem.* **1996**, *409*, 9.
(47) Sanchez, C.; Leiva, E.; Dannie, S.; Baruzzi, A. *Bull. Chem. Soc. Jpn.* **1998**, *71*, 549.
(48) Osakay, T.; Ogata, A.; Ebina, K. *J. Phys. Chem.* **1997**, *101*, 8341.
(49) Rais, J.; Kyrs, M.; Pivonková, M. *J. Inorg. Nucl. Chem.* **1968**, *30*, 611.
(50) Motomizu, S.; Tôei, K.; Iwashido, T. *Bull. Chem. Soc. Jpn.* **1969**, *42*, 1006.
(51) Kawasaki, M.; Tôei, K.; Iwashido, T. *Chem. Lett.* **1972**, 417.
(52) Iwashido, T.; Minami, M.; Kimura, M.; Sadakani, A.; Kawasaki, M.; Tôei, K. *Bull. Chem. Soc. Jpn.* **1980**, *53*, 703.
(53) Yamamoto, Y.; Tarumoto, T.; Tarui, T. *Chem. Lett.* **1972**, 459.
(54) Kenjo, T.; Diamond, R. *J. Phys. Chem.* **1972**, *76*, 2454.
(55) Kenjo, T.; Diamond, R. *J. Inorg. Nucl. Chem.* **1974**, *36*, 183.
(56) Kusakabe, S.; Shinoda, M.; Kusafuka, K. *Bull. Chem. Soc. Jpn.* **1989**, *62*, 333.
(57) Kusakabe, S.; Arai, M. *Bull. Chem. Soc. Jpn.* **1996**, *69*, 581.
(58) Schweighofer, K.; Benjamin, I. *J. Phys. Chem.* **1995**, *99*, 9974.